

A High-Order NVD/TVD-Based Polynomial Upwind Scheme for the Modified Burgers' Equations

Wei Gao^{1,*}, Yang Liu¹, Bin Cao¹ and Hong Li¹

¹ School of Mathematical Sciences, Inner Mongolia University, Huhhot, P. R. China

Received 19 February 2011; Accepted (in revised version) 9 November 2011

Available online 30 July 2012

Abstract. A bounded high order upwind scheme is presented for the modified Burgers' equation by using the normalized-variable formulation in the finite volume framework. The characteristic line of the present scheme in the normalized-variable diagram is designed on the Hermite polynomial interpolation. In order to suppress unphysical oscillations, the present scheme respects both the TVD (total variational diminishing) constraint and CBC (convection boundedness criterion) condition. Numerical results demonstrate the present scheme possesses good robustness and high resolution for the modified Burgers' equation.

AMS subject classifications: 65M08, 76M12

Key words: modified Burgers' equation, TVD, NVD, upwind scheme.

1 Introduction

The modified Burgers' equation (MBE) has the form as follows

$$\frac{\partial u}{\partial t} + u^m \frac{\partial u}{\partial x} = \nu \frac{\partial^2 u}{\partial x^2}, \quad a \leq x \leq b, \quad t \geq t_0, \quad (1.1)$$

where m is a positive integer with $m \geq 1$. The case with $m = 1$ is the so-called viscous Burgers' equation which is the fundamental equation in fluid dynamics. The MBE equation possesses the strongly nonlinear terms in the governing equation modeling many practical transport problems such as ion reflection at quasi-perpendicular shocks, nonlinear waves in a medium with low-frequency pumping or absorption, wave processes in thermoelastic media, turbulence transport, transport and dispersion of pollutants in rivers and sediment transport, etc. Recent researches on the

*Corresponding author.

Email: mathgao@mail.ustc.edu.cn (W. Gao), mathliuyang@yahoo.cn (Y. Liu), bincao@gmail.com (B. Gao), smslh@imu.edu.cn (H. Li)

theoretical analysis of the MBE equation can be found in the references [1–4]. Meanwhile, numerical solutions of the MBE equations were performed by using the collection method [5], the B-spline finite element methods [6, 7], the B-spline collocation methods [8–11], the El-Gendi method [12], the Lattice Boltzmann method [13] and the fourth-order compact scheme [14].

One of key issues in the numerical solution of the MBE equation is the discretization of the strongly nonlinear convection term $u^m \partial u / \partial x$. Stable and bounded convection schemes are usually used to guarantee the numerical solutions convergent to the physical solutions. Despite the well-known lower-order schemes, such as the first-order upwind (FOU) and Power-law scheme, are unconditionally bounded and stable, they may often generate unsatisfactory numerical diffusion to smear the computed solutions. To remedy this defect, second-order and higher-order schemes, such as the central difference (CD), second-order upwind (SOU) [15], quadratic upstream interpolation for convective kinematics (QUICK) [16], cubic upwind interpolation (CUI) [17, 18] and Lax-Wendroff [19], were proposed for the approximation of the convection terms. However, none of these linear high-order (HO) schemes possess boundedness according to the Godunov's order barrier theorem [20]. They tend to cause unphysical oscillations in the vicinity of steep gradients and discontinuities, which would destroy numerical results and lead to numerical instability.

Combination of a boundedness property with the HO schemes produces the high-resolution (HR) schemes [21, 22]. The HR schemes can provide good resolution of steep gradients and discontinuities without introducing excessive numerical diffusion and unphysical oscillations in the solution. One of the principal boundedness criteria is the total variational diminishing (TVD) constraint proposed by Harten [21]. Based on the TVD constraint, the limiter function presented by Sweby [22] and Roe [20] are introduced to ensure the boundedness of the numerical schemes. Many limiter functions were proposed since then, such as MINMOD by Sweby [22], SUPERBEE by Roe [20] and MUSCL by van Leer [23, 24] and so on. Another significant technique is the convection boundedness criterion (CBC) by Gaskell and Lau [25] by using the normalized variable (NV) formulation of Leonard [26]. Numerical schemes satisfying the CBC is to be of the convection boundedness. From then on, many schemes were presented by using the CBC condition, such SMART [25], CLAM [27], STOIC [28], HOAB [29], WACEB [30], CUBISTA [45] and so on. Further researches by Yu *et al.* [32], Wei *et al.* [29] and Hou *et al.* [33] indicated that the CBC of Gaskell and Lau focused only on the boundedness and paid no attention to any restriction of the accuracy. To remedy this drawback, Wei *et al.* [29] and Hou *et al.* [33] proposed an improved edition named the BAIR condition (Boundedness, Accuracy and Interpolative Reasonableness) to guarantee both boundedness and high accuracy of the convection schemes. The CBC and BAIR are basically used to design the bounded schemes for the incompressible flows and steady problems. In contrast to the TVD schemes, the CBC schemes may be unbounded in simulating some specific problems like the shock tube flows although they work well in the passive scalar problems [34, 35]. In spite of this, the HR schemes can be easily constructed in the normalized variable formulation

(NVF) by translating the CBC or BAIR condition into the CBC region in the normalized variable diagram (NVD).

The aim of the present paper is to design a high-order bounded schemes satisfying both the TVD constraint and BAIR condition for the solutions of the modified Burgers' equations. The smooth characteristic line of the present scheme is designed on the Hermite polynomial interpolation in the NV diagram. Numerical results demonstrates the present scheme possesses high resolution for the nonlinear modified Burgers' equations.

2 Two Boundedness criteria and the NV formulation

The letters U, C, D and f in Fig. 1 denote the upwind, central, downwind mesh point and the cell face on the uniform mesh, respectively. The cell-face value of the convected variable can be predicted by using the so-called κ -scheme. The generic formulation of the κ -scheme can be written as

$$\phi_f = \phi_C + [\frac{1+\kappa}{4}(\phi_D - \phi_C) + \frac{1-\kappa}{4}(\phi_C - \phi_U)], \tag{2.1}$$

where the parameter $\kappa \in [-1, 1]$ is to be chosen. Several well-known linear high-order convection schemes are listed in Table 1 by setting different values of κ . According to Leonard [26], the original variable ϕ can be normalized on the uniform mesh by

$$\hat{\phi} = \frac{\phi - \phi_U}{\phi_D - \phi_U}, \tag{2.2}$$

Using this notation, the κ -schemes (2.1) can be reformed as

$$\hat{\phi}_f = (1 - \frac{1}{2}\kappa)\hat{\phi}_C + \frac{1}{4}(1 + \kappa), \tag{2.3}$$

which states that the normalized cell-face value $\hat{\phi}_f$ depends only on the value $\hat{\phi}_C$. The NV formulations of the mentioned linear convection schemes are listed in Table 1. It is noted that none of them is bounded. All of these linear schemes with at least second-order accuracy have to suffer from unphysical oscillations in the vicinity of discontinuities and steep gradients in the solution, as predicted by the Godunov's theorem [36]. Thus, some a boundedness criterion is to be combined with the linear high-order schemes to design the bounded high-resolution schemes.

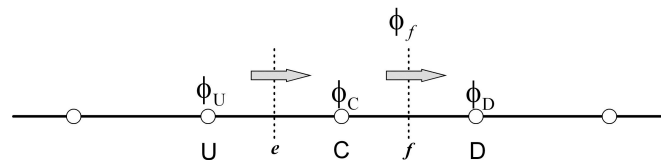


Figure 1: The cell face and three neighboring points for the normalized variable formulation

Table 1: The linear convection schemes and the NV formulations.

Schemes	κ	Non-Normalized	Normalized
SOU	-1	$\phi_f = \frac{3}{2}\phi_C - \frac{1}{2}\phi_U$	$\hat{\phi}_f = \frac{3}{2}\hat{\phi}_C$
CD	1	$\phi_f = \frac{1}{2}\phi_C + \frac{1}{2}\phi_D$	$\hat{\phi}_f = \frac{1}{2}\hat{\phi}_C + \frac{1}{2}$
Fromm	0	$\phi_f = \phi_C + \frac{1}{4}(\phi_D - \phi_U)$	$\hat{\phi}_f = \hat{\phi}_C + \frac{1}{4}$
QUICK	$\frac{1}{2}$	$\phi_f = \frac{3}{4}\phi_C + \frac{3}{8}\phi_D - \frac{1}{8}\phi_U$	$\hat{\phi}_f = \frac{3}{8} + \frac{3}{4}\hat{\phi}_C$
CUI	$\frac{1}{3}$	$\phi_f = \frac{5}{6}\phi_C + \frac{1}{3}\phi_D - \frac{1}{6}\phi_U$	$\hat{\phi}_f = \frac{5}{6}\hat{\phi}_C + \frac{1}{3}$

Gaskell and Lau [25] proposed the CBC for convection discretization to possess the boundedness. The CBC is defined mathematically in the NV formulation by the following conditions

$$\begin{cases} \hat{\phi}_C \leq \hat{\phi}_f = f(\hat{\phi}_C) \leq 1, & \text{if } 0 < \hat{\phi}_C < 1, \\ \hat{\phi}_f = \hat{\phi}_C, & \text{if } \hat{\phi}_C \geq 1, \\ \hat{\phi}_f = \hat{\phi}_C, & \text{if } \hat{\phi}_C \leq 0. \end{cases} \quad (2.4)$$

As shown in Fig. 2, the shaded area and the line passing through the points (0, 1) and (1, 1) consists in the CBC region. Afterwards, Wei et al. [29] and Hou et al. [33] proposed the BAIR (Boundedness, Accuracy and Interpolative Reasonableness) as the sufficient and necessary condition to assure both the boundedness and at least second-order accuracy of the convection schemes. The BAIR condition can be mathematically written as

$$\begin{cases} \frac{3}{2}\hat{\phi}_C \leq f(\hat{\phi}_C) \leq \frac{1}{2}(\hat{\phi}_C + 1), & \text{if } 0 < \hat{\phi}_C < \frac{1}{2}, \\ \frac{1}{2}(\hat{\phi}_C + 1) \leq f(\hat{\phi}_C) \leq \frac{3}{2}\hat{\phi}_C \text{ and } f(\hat{\phi}_C) \leq 1, & \text{if } \frac{1}{2} \leq \hat{\phi}_C < 1, \\ \hat{\phi}_f = \hat{\phi}_C, & \text{if } \hat{\phi}_C \geq 1, \\ \hat{\phi}_f = \hat{\phi}_C, & \text{if } \hat{\phi}_C \leq 0. \end{cases} \quad (2.5)$$

Fig. 2 illustrates the relationship of the CBC and BAIR, which shows that the convection scheme obeying the BAIR have to be the CBC scheme, but not vice versa.

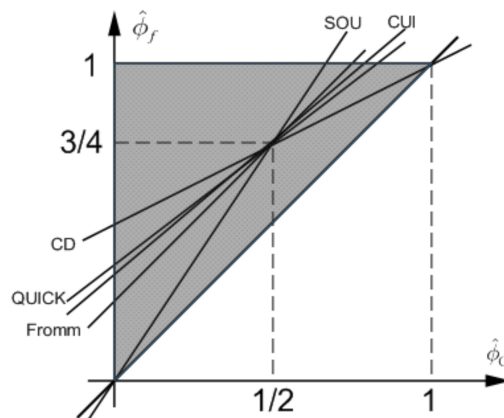


Figure 2: The relationship of the CBC region and the characteristic lines of the linear HO schemes.

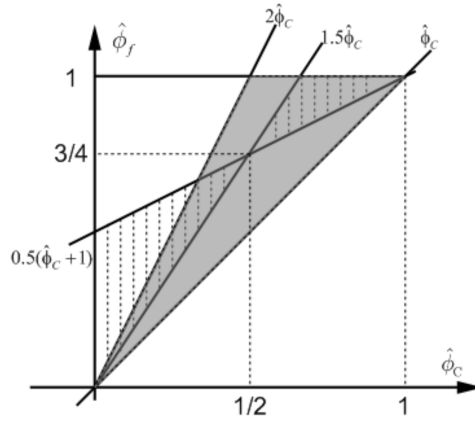


Figure 3: The TVD (shaded) and CBC-BAIR (hatched) regions.

Another important boundedness criterion for the convection treatment is the total variational diminishing (TVD) constraint by Harten [21]. The TVD constraint can guarantee that the numerical solution of the conservative scheme is free from the spurious oscillations and convergent to the weak solution of the conservation law. In summary, the total variation of a numerical solution $\{\phi_i\}$ is defined by

$$TV(\phi) = \sum_i |\phi_{i+1} - \phi_i|, \tag{2.6}$$

and a numerical scheme is said to be TVD if it satisfies

$$TV(\phi^{n+1}) \leq TV(\phi^n). \tag{2.7}$$

It is noted that the TVD constraint was converted by Sweby [22] to a set of restrictions as follows

$$0 \leq \Psi(r) \leq \min(2r, 2), \quad \text{for } r > 0, \tag{2.8a}$$

$$\Psi(r) = 0, \quad \text{for } r \leq 0, \tag{2.8b}$$

where $\Psi(r)$ is the limiter function and r expresses a local gradient ratio defined as

$$r = \left(\frac{\partial\phi}{\partial x}\right)_e / \left(\frac{\partial\phi}{\partial x}\right)_f, \tag{2.9}$$

where r is simplified on the uniform mesh as

$$r = \frac{\phi_C - \phi_U}{\phi_D - \phi_C}, \tag{2.10}$$

and the NV formulation reads as follows

$$r = \frac{\hat{\phi}_C}{1 - \hat{\phi}_C}. \tag{2.11}$$

From these equations, the set of the TVD constraints can be rewritten in the NV formulation as

$$\begin{aligned}\hat{\phi}_f &\leq 1, \quad \text{and} \quad \hat{\phi}_f \in [\hat{\phi}_C, 2\hat{\phi}_C], \quad 0 < \hat{\phi}_C < 1, \\ \hat{\phi}_f &= \hat{\phi}_C, \quad \hat{\phi}_C \geq 1, \\ \hat{\phi}_f &= \hat{\phi}_C, \quad \hat{\phi}_C \leq 0.\end{aligned}\tag{2.12}$$

The shaded area in Fig. 3 depicts the relationship between the TVD constraint and the BAIR condition. After the convection scheme was presented in the NV formulation, its corresponding limiter formulation can be also obtained by reforming its corresponding NV formulation in the following equation

$$\hat{\phi}_f = \hat{\phi}_C + \frac{1}{2}\Psi(r)(1 - \hat{\phi}_C).\tag{2.13}$$

It is observed in Figs. 2 and 3 that the characteristic lines of all the well-known linear HO schemes go beyond the CBC (BAIR) and TVD regions in the NV diagram. It is shown that neither the BAIR condition nor the TVD constraint holds for these linear HO schemes.

3 Method

The generic form of the nonlinear HR scheme for the convection variable in the NV formulation can be written as

$$\hat{\phi}_f = f(\hat{\phi}_C).\tag{3.1}$$

The following two properties hold for such schemes according to the Zijlema and Wesseling's conclusions [38].

- A characteristic line of a convection scheme in the NV diagram passing through the point $(1/2, 3/4)$ has second-order local truncation error.
- A characteristic line of a convection scheme in the NV diagram satisfying

$$f\left(\frac{1}{2}\right) = \frac{3}{4}, \quad f'\left(\frac{1}{2}\right) = 1 - \frac{1}{2}\kappa,$$

possesses the same formal order of accuracy as the corresponding κ -scheme.

- A characteristic line of $f(\hat{\phi}_C)$ should be located into the TVD or CBC region for $\hat{\phi}_C \in (0, 1)$.

Consequently, the smooth characteristic line of the proposed scheme needs to satisfy the following condition

- It passes through three points $(0, 0)$, $(1/2, 3/4)$ and $(1, 1)$ for $\hat{\phi}_C \in (0, 1)$.
- $f'(0) = \theta_1$, $f'\left(\frac{1}{2}\right) = 1 - \frac{1}{2}\kappa$, $f'(1) = \theta_2$.

Under this line, we employ the Hermite interpolation to design a five-degree polynomial as the characteristic line of the proposed scheme.

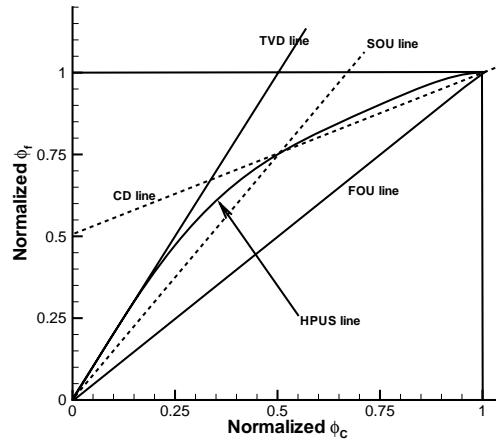


Figure 4: The illustration of the NV line of the HPUS scheme in the BAIR region.

κ is set to $1/2$ so that the proposed scheme can mimic the performance of the QUICK scheme which possesses the third-order accuracy to approximating the cell face value according to Leonard’s recommendations [26]. As shown in Fig. 3, the ranges of the parameters θ_1 and θ_2 hold

$$\frac{3}{2} \leq \theta_1 \leq 2, \quad 0 \leq \theta_2 \leq \frac{1}{2},$$

so that the proposed scheme can respect both the TVD and BAIR. The present scheme takes $\theta_1 = 2$ and $\theta_2 = 0$. In view of the above mentioned analysis, the proposed HPUS scheme (high-order Hermite polynomial upwind scheme, HPUS) is given in the NV formulation by

$$\hat{\phi}_f = \begin{cases} \hat{\phi}_C(-4\hat{\phi}_C^4 + 10\hat{\phi}_C^3 - 8\hat{\phi}_C^2 + \hat{\phi}_C + 2), & 0 < \hat{\phi}_C < 1, \\ \hat{\phi}_C, & \text{elsewhere.} \end{cases} \quad (3.2)$$

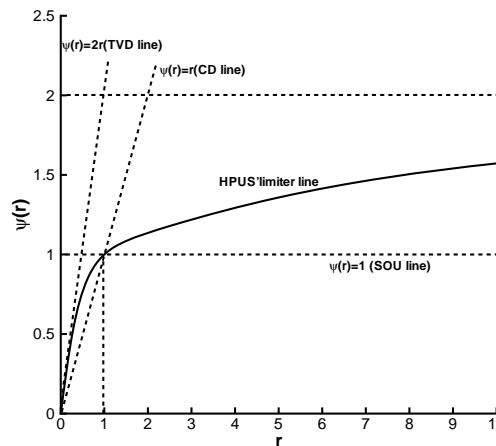


Figure 5: The illustration of the flux limiter of the HPUS scheme in the Sweby second-order TVD region.

Furthermore, the limiter function of the HPUS scheme is yielded according to Eqs. (2.11) and (3.2) as follows

$$\Psi(r) = \max\left\{0, \frac{(|r| + r)(r^3 + r^2 + 5r + 1)}{(1 + |r|)^4}\right\}. \quad (3.3)$$

The characteristic line of the HPUS scheme in the NV diagram is plotted in Fig. 4, which shows that the HPUS scheme respects the TVD and BAIR. Additionally, the profile of the HPUS's limiter function depicted in Fig. 5 demonstrates that it falls into the Sweby's second-order TVD region, which indicates that the convection schemes based on both the TVD constraint and BAIR condition can lead to the second-order TVD scheme. The detailed description of the present algorithm can be found in 'Appendix'.

4 Numerical results and discussions

4.1 Linear equations

The linear advection equation is one of the simplest hyperbolic conservation laws. It describes the transport of the scalar quantity u with the constant characteristic speed a . This equation can be written as

$$\frac{\partial u}{\partial t} + a \frac{\partial u}{\partial x} = 0, \quad (4.1)$$

we solve the advection equation (4.1) with a smooth initial distribution described by

$$u(x, 0) = \sin^4(\pi x), \quad (4.2)$$

on the computational domain $[-1, 1]$. This test case is employed to the spatial accuracy of the HPUS scheme. The periodic boundary condition is adopted for simple implementation of the numerical scheme. The computations are performed on the uniform meshes with 20, 40, 80, 160 and 320 cells, respectively. Three norms are defined as follows to measure the errors [44]

$$\begin{aligned} \|E\|_{L_p} &= \frac{\sum_{i=1}^N |\bar{u}_i(\text{computed}) - \bar{u}_i(\text{exact})|^p}{N}, \quad p = 1, 2, \\ \|E\|_{L_\infty} &= \max_{1 \leq i \leq N} |\bar{u}_i(\text{computed}) - \bar{u}_i(\text{exact})|. \end{aligned} \quad (4.3)$$

The order of accuracy can be calculated by the equation

$$\text{order} = \frac{\log E_N / E_{2N}}{\log 2}. \quad (4.4)$$

The L_1 , L_2 and L_∞ errors are demonstrated in Table 2, as well as the corresponding accuracy orders. It is seen from the table that the accuracy order of the HPUS

Table 2: L_1 , L_2 and L_∞ errors and orders of HPUS for the advection equation with the smooth initial distribution: $u(x, 0) = \sin^4(\pi x)$.

Scheme	Mesh	L_1 error	L_1 order	L_2 error	L_2 order	L_∞ error	L_∞ order
HPUS	20	1.712e-2	—	2.824e-2	—	7.746e-2	—
	40	4.416e-3	1.94	7.620e-3	1.89	1.951e-2	1.99
	80	9.161e-4	2.27	1.494e-3	2.35	4.397e-3	2.15
	160	1.677e-4	2.45	2.678e-4	2.48	8.503e-4	2.37
	320	2.469e-5	2.76	3.810e-5	2.81	1.300e-4	2.71
HOAB	20	1.710e-2	—	2.382e-2	—	5.915e-2	—
	40	5.596e-3	1.62	7.480e-3	1.68	1.716e-2	1.79
	80	1.764e-3	1.67	2.403e-3	1.66	7.403e-3	1.22
	160	4.711e-4	1.91	7.568e-4	1.67	3.109e-3	1.26
	320	1.203e-4	1.98	2.329e-4	1.71	1.355e-3	1.20
SMART	20	1.472e-2	—	2.444e-2	—	6.916e-2	—
	40	3.347e-3	2.15	6.171e-3	1.99	2.480e-2	1.48
	80	8.367e-4	2.01	1.667e-3	1.90	8.685e-3	1.52
	160	2.162e-4	1.96	4.746e-4	1.82	3.044e-3	1.52
	320	5.255e-5	2.05	1.348e-4	1.82	1.062e-3	1.53

scheme approximates 3 on three relevant norms, which mimics the performance of the QUICK scheme as expected. We compare the HPUS scheme with another two schemes, SMART [25], and HOAB [29]. It is seen that the accuracy order of HPUS is better than that of SMART and HOAB as the mesh is refined. It is noted that for the L_∞ order, the HOAB scheme perform markedly worse than another three schemes. This phenomenon may result from the fact that the HOAB scheme is the hybrid schemes which have the slope change at the point (0.5, 0.75) in the NV formulation [45, 46].

4.2 The Burgers' equation (m=1)

Owing to possessing the nonlinear convection and linear diffusion, the Burgers' equation is always regarded as a significant case to the verification of the numerical scheme. A typical initial distribution is specified by

$$u(x, 0) = u_0(x) = \sin(\pi x), \tag{4.5}$$

and the periodic boundary condition reads as

$$u(0, t) = u(1, t) = 0. \tag{4.6}$$

The exact Fourier solution is given by

$$u(x, t) = 2\pi v \frac{\sum_{n=1}^{\infty} a_n \exp(-n^2 \pi^2 v t) n \sin(n \pi x)}{a_0 + \sum_{n=1}^{\infty} a_n \exp(-n^2 \pi^2 v t) \cos(n \pi x)}, \tag{4.7}$$

where the Fourier coefficients are

$$a_0 = \int_0^1 \exp(-(2\pi v)^{-1}(1 - \cos(\pi x))) dx, \tag{4.8}$$

$$a_n = \int_0^1 \exp(-(2\pi v)^{-1}(1 - \cos(\pi x))) \cos(n \pi x) dx.$$

Table 3: Comparison of the numerical and exact solutions at ten points for the Burgers' equation with $\nu = 1.0$ at $t = 0.1$.

x	numerical solutions on different meshes				Exact
	$N = 20$	$N = 40$	$N = 80$	$N = 160$	
0.1	0.10969	0.10942	0.10955	0.10954	0.10954
0.2	0.21019	0.20956	0.20981	0.20980	0.20979
0.3	0.29236	0.29158	0.29193	0.29190	0.29190
0.4	0.34851	0.34755	0.34796	0.34793	0.34792
0.5	0.37223	0.37118	0.37162	0.37159	0.37158
0.6	0.35976	0.35867	0.35909	0.35906	0.35905
0.7	0.31059	0.30959	0.30995	0.30992	0.30991
0.8	0.22835	0.22759	0.22785	0.22783	0.22782
0.9	0.12098	0.12057	0.12071	0.12069	0.12069

Table 4: Comparison of the numerical solution at different times for the Burgers' equation with $\nu = 0.01$.

x	t	numerical solutions by different schemes				Exact
		Hassanien [39]	Kutluay [40]	Xu [41]	HPUS	
0.25	0.4	0.3419	0.3424	0.3419	0.3419	0.3419
	0.6	0.2690	0.2691	0.2689	0.2690	0.2690
	0.8	0.2215	0.2215	0.2215	0.2215	0.2215
	1.0	0.1881	0.1881	0.1882	0.1882	0.1882
	3.0	0.0751	0.0751	0.0751	0.0751	0.0751
0.50	0.4	0.6607	0.6715	0.6607	0.6608	0.6607
	0.6	0.5294	0.5341	0.5294	0.5294	0.5294
	0.8	0.4391	0.4414	0.4391	0.4391	0.4391
	1.0	0.3744	0.3757	0.3744	0.3744	0.3744
	3.0	0.1522	0.1502	0.1502	0.1502	0.1502
0.75	0.4	0.9103	0.9468	0.9103	0.9104	0.9103
	0.6	0.7672	0.7847	0.7672	0.7673	0.7672
	0.8	0.6474	0.6566	0.6474	0.6474	0.6474
	1.0	0.5561	0.5614	0.5560	0.5561	0.5561
	3.0	0.2248	0.2250	0.2248	0.2248	0.2248

Table 5 lists the numerical solutions at ten selected points for the viscosity $\nu = 1.0$ at $t = 0.1$. Compared to the exact solutions, it can be seen that the considerably accurate results are obtained on the mesh size $h = 1/160$. For the case with $\nu = 0.01$ at different five time instants, numerical results were obtained by using the forth-order difference scheme by Hassanien et al. [39], the explicit difference scheme by Kutluay et al. [40] and the B-spline scheme by Xu et al. [41]. Table 4 shows comparison between

Table 5: Comparisons of results by the different schemes for the modified Burgers' equation with $m = 2$ and $\nu = 0.005$ at four time instants.

$\nu = 0.005$	$t = 2$		$t = 4$		$t = 6$		$t = 10$	
	$L_2 \times 10^3$	$L_\infty \times 10^3$						
HPUS	0.22672	0.58119	0.18776	0.42987	0.16412	0.33007	0.13917	0.22889
[5]	0.25786	0.72264	0.25277	0.55445	0.22569	0.43082	0.18735	0.30006
[10]	0.22651	0.57998	0.18816	0.42940	0.16460	0.32897	0.13959	0.22885
[14]	0.22653	0.58027	0.18819	0.42949	0.16461	0.32993	0.13524	0.22874

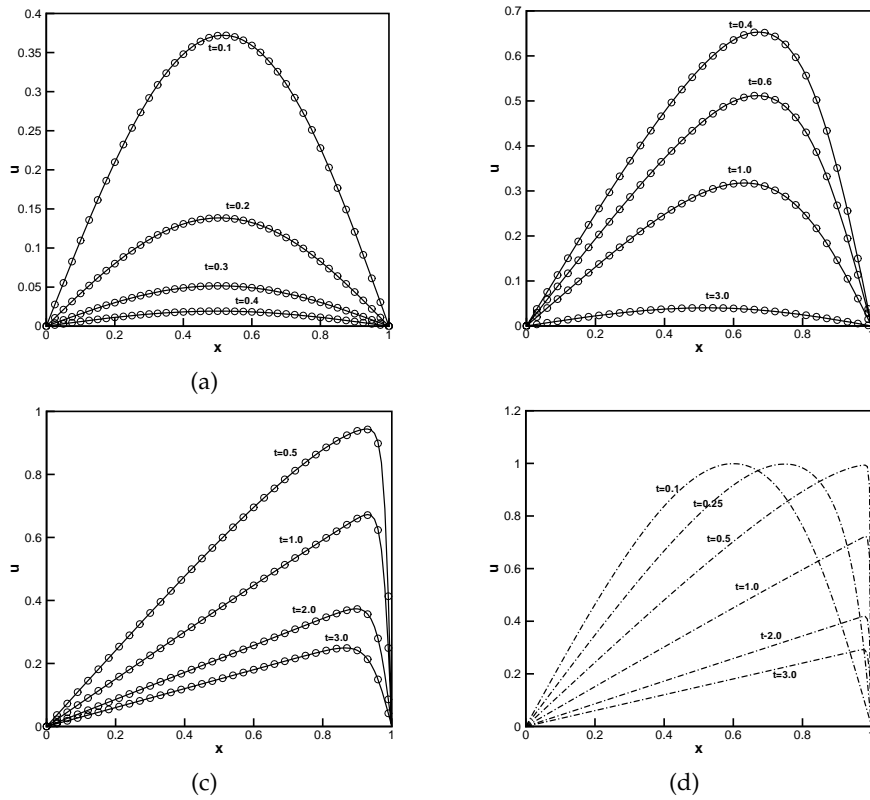


Figure 6: Comparison of numerical (circled lines) and exact (solid lines) solutions for the Burgers' equation with different viscosity coefficients at selected time instants: (a) $\nu = 1.0$ (b) $\nu = 0.1$ (c) $\nu = 0.01$. The dashed line in (d) denotes the numerical solution for $\nu = 0.001$ at several time instants.

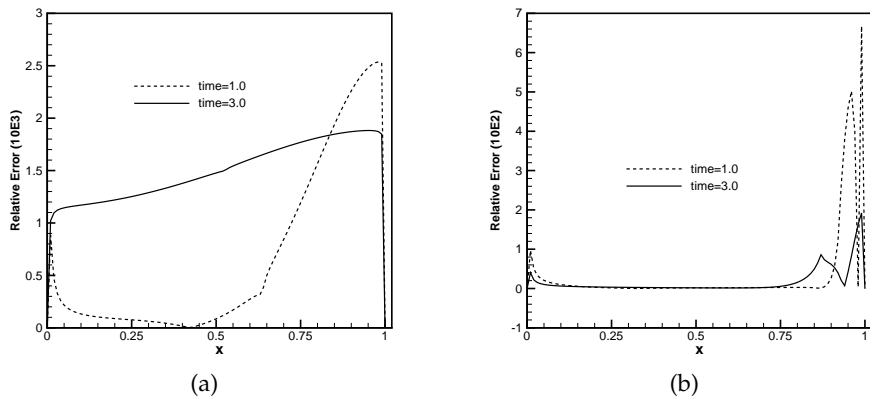


Figure 7: Computed relative errors: (a) $\nu = 0.1$ (b) $\nu = 0.01$.

the present results and referenced results on the mesh size $h = 1/100$. It is concluded that the numerical solutions by the second-order HPUS scheme are as good as the ones by the higher-order schemes [39,41] on the same mesh size. The present scheme possesses better efficiency than the compared schemes. Figs. 8(a)-6(c) demonstrate the curves of both the numerical and exact solutions for $\nu = 1.0, 0.1, 0.01$ at different

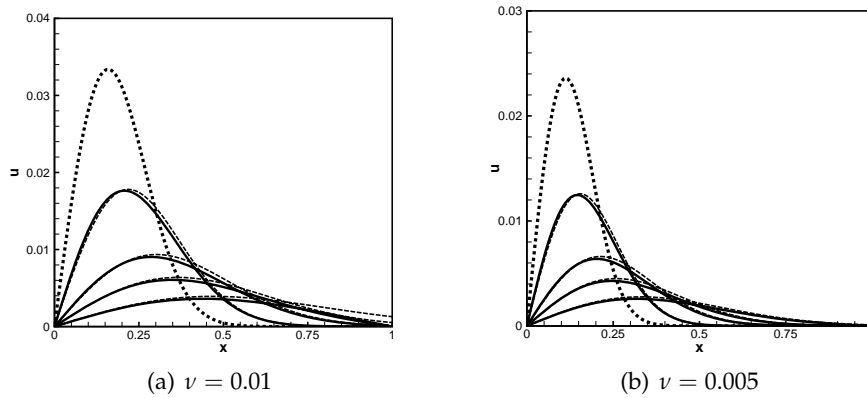


Figure 8: The exact (solid) and numerical (dotted) solution profiles for the modified Burgers' equation with $m = 2$ at various time instants. The highest dashed curves show the exact initial solutions at $t = 1$.

time instants, respectively. These plots show that the numerical solutions are in good agreement with the exact ones. For the case of $\nu = 0.001$, the curves of the numerical solutions are plotted in Fig. 6(d) since the Fourier series solution is not available for $\nu < 0.01$ due to its slow convergence. It can be seen that the numerical solution curves show the correct physical behavior in this case. Fig. 7 plots the relative errors of the test case with $\nu = 0.1$ and $\nu = 0.01$ at two selected time instants, respectively. The smaller relative errors are obtained for the test case with the higher viscosity. The higher values of the relative error appear near the boundary layer especially for the smaller viscosity.

4.3 The MBE (m=2)

The modified Burgers' equation with $m = 2$ has the exact solution as follows

$$u(x, t) = \frac{x}{t} \left[1 + \frac{\sqrt{t}}{t_0} \exp\left(\frac{x^2}{4\nu t}\right) \right]^{-1}, \quad 0 \leq x \leq 1, \quad t \geq t_0, \quad (4.9)$$

with the constant prescribed as 0.5 in this case. The computation interval is set to $[0, 1]$. The initial distribution is obtained by setting the equation (4.9) at the time $t=1$. The mesh size equals $1/1000$. The absolute errors between the numerical and exact solutions are computed for two different values of the viscosity, $\nu = 0.005, 0.01$ and measured by using the L_2 norm and the L_∞ norm, respectively. In Tables 5 and 6, the computed errors by the HPUS scheme are compared to the ones published in the

Table 6: Comparisons of results by the different schemes for the modified Burgers' equation with $m = 2$ and $\nu = 0.01$ at four time instants.

$\nu = 0.01$	$t = 2$		$t = 4$		$t = 6$		$t = 10$	
	$L_2 \times 10^3$	$L_\infty \times 10^3$						
HPUS	0.37892	0.81778	0.31645	0.60575	0.32533	0.52579	0.54627	1.28123
[5]	0.52308	1.21698	0.51625	0.93136	0.49023	0.72249	0.64007	1.28124
[10]	0.37932	0.81680	0.31724	0.60537	0.32602	0.52579	0.54701	1.28125
[14]	0.37920	0.81669	0.31548	0.60556	0.27314	0.46499	0.19337	0.30183

references [5, 10, 14]. The comparisons demonstrate that under the same mesh, the present results agree well with the ones by the higher-order schemes in [10, 14] and are much better than the ones in [5]. Fig. 8 illustrates the exact and numerical solution profiles for $\nu = 0.005, 0.01$ at various time instants. It can be observed that the difference between the exact and numerical profiles gets to be indistinguishable as the time increases.

4.4 The MBE (m=3)

The modified equation with $m = 3$ is solved by using the following initial condition

$$u(x, 0) = A \sin\left(\frac{\pi x}{d}\right), \tag{4.10}$$

where the parameters $A = 1$ and $d = \pi$. It has an asymptotic solution of the form

$$u(x, t) = e^{-kt} f_0(x, t) + e^{-4kt} f_1(x, t) + e^{-7kt} f_2(x, t) + \dots, \tag{4.11}$$

where the old age constant $A_1 = 0.365366$ and

$$f_0(x, t) = A_1 \sin\left(\frac{\pi x}{d}\right), \tag{4.12a}$$

$$f_1(x, t) = -\frac{A_1^4 \pi}{4d} t \sin\left(\frac{2\pi x}{d}\right) + \frac{A_1^4 d}{96\nu\pi} \sin\left(\frac{4\pi x}{d}\right) = B_1 t \sin\left(\frac{2\pi x}{d}\right) + B_2 \sin\left(\frac{4\pi x}{d}\right), \tag{4.12b}$$

$$f_2(x, t) = g_3(t) \sin\left(\frac{\pi x}{d}\right) + g_4(t) \sin\left(\frac{3\pi x}{d}\right) + g_5(t) \sin\left(\frac{5\pi x}{d}\right) + g_6(t) \sin\left(\frac{7\pi x}{d}\right), \tag{4.12c}$$

$$g_3(t) = -\frac{d^2}{6\nu\pi^2} [D_1 t + E_1 + \frac{d^2 D_1}{6\nu\pi^2}], \quad g_4(t) = \frac{d^2}{2\nu\pi^2} [D_2 t + E_2 - \frac{d^2 D_2}{2\nu\pi^2}] \tag{4.12d}$$

$$g_5(t) = \frac{d^2}{18\nu\pi^2} [D_3 t + E_3 - \frac{d^2 D_3}{18\nu\pi^2}], \quad g_6(t) = \frac{d^2 E_4}{42\nu\pi^2} \tag{4.12e}$$

$$D_1 = \frac{A_1^3 B_1 \pi}{4d}, \quad D_2 = -\frac{9A_1^3 B_1 \pi}{8d}, \quad D_3 = \frac{5A_1^3 B_1 \pi}{8d} \tag{4.12f}$$

$$E_1 = \frac{A_1^3 B_2 \pi}{8d}, \quad E_2 = \frac{9A_1^3 B_2 \pi}{8d}, \quad E_3 = -\frac{15A_1^3 B_1 \pi}{8d} \tag{4.12g}$$

$$E_4 = \frac{7A_1^3 B_2 \pi}{8d}, \quad k = \frac{\nu\pi^2}{d^2} \tag{4.12h}$$

In Table 7, the absolute errors of results by the HPUS scheme are compared to the ones in [13, 14] at seven selected time instants for $\nu = 0.005$ and the mesh size $h = 1/200$. It

Table 7: Comparisons of results by the different schemes for the modified Burgers' equation with $m = 3$ and $\nu = 0.005$ at four time instants.

$\nu = 0.005$		150	200	250	300	350	400	450
HPUS	L_2	0.3403e-02	0.1157e-02	0.4292e-03	0.1585e-03	0.5828e-04	0.2145e-04	0.8000e-05
	L_∞	0.6697e-02	0.1836e-02	0.6340e-03	0.2294e-03	0.8289e-04	0.3180e-04	0.1269e-04
[13]	L_2	0.3227e-02	0.9912e-03	0.5031e-03	0.5939e-03	0.6940e-02	0.7567e-03	0.7990e-03
	L_∞	0.5172e-02	0.1671e-02	0.1400e-02	0.1452e-02	0.1488e-02	0.1513e-02	0.1531e-02
[14]	L_2	0.6126e-02	0.2227e-02	0.9124e-03	0.4134e-03	0.2307e-03	0.1617e-03	0.1284e-03
	L_∞	0.6840e-02	0.2042e-02	0.8335e-03	0.3956e-03	0.2186e-03	0.1416e-03	0.1036e-03

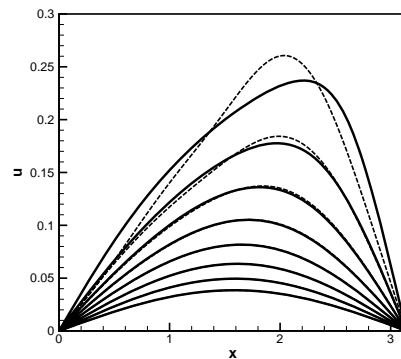


Figure 9: The exact (solid) and numerical (dashed) solution profiles for the modified Burgers' equation with $m = 3$ at seven selected time instants.

can be seen that the present results are much better than the ones by the fourth-order scheme in [14] and the LBM method in [13] despite that the HPUS scheme is of second-order accuracy. In Fig. 9, no difference between the exact and numerical profiles can be indistinguished for the time $t \geq 250$.

5 Conclusion

A bounded high-order upwind scheme in the normalized-variable formulation is constructed for the numerical solution of the modified Burgers' equations. The characteristic line of the present scheme in the normalized-variable diagram is designed by using the Hermite polynomial. The TVD constraint is combined with the CBC-BAIR condition to keep the present HPUS scheme free from the unphysical oscillations. The numerical results are performed for the modified Burgers' equations with $m = 1, 2, 3$, respectively. Comparisons with the published results demonstrate that the HPUS scheme possesses satisfactory accuracy and good efficiency for the nonlinear modified Burgers' equations.

Appendix

The model equation for the modified Burgers' equations can be written in a generic form as

$$\frac{\partial u}{\partial t} + \frac{\partial f(u)}{\partial x} = \nu \frac{\partial^2 u}{\partial x^2}. \quad (5.1)$$

The flux $f(u) = au$ presents the linear advection equation and $f(u) = u^{m+1}/(m+1)$ presents modified Burgers' equations. The HPUS scheme is associated with the cell-centered mesh as plotted in Fig. 10. By integrating on the cell $[x_{i-1/2}, x_{i+1/2}]$, the model equation (5.1) can be reformed as

$$\frac{d\bar{u}(x_i, t)}{dt} = -\frac{1}{\Delta x} \left(f(u(x_{i+1/2}, t)) - f(u(x_{i-1/2}, t)) \right) + \nu \left(u'(x_{i+1/2}, t) - u'(x_{i-1/2}, t) \right), \quad (5.2)$$

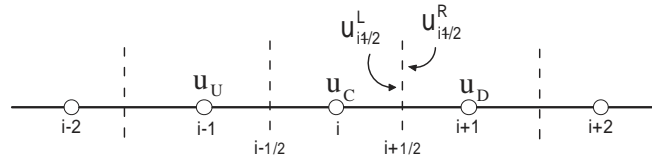


Figure 10: The cell-centered mesh for the numerical computation.

where

$$\bar{u}_i(t) = \frac{1}{\Delta x} \int_{x_{i-\frac{1}{2}}}^{x_{i+\frac{1}{2}}} u(\xi, t) d\xi,$$

is the cell average of the function $u(x, t)$. We approximate (5.2) by the following conservation scheme

$$\frac{d\bar{u}_i(t)}{dt} = -\frac{1}{\Delta x} (\hat{f}_{i+\frac{1}{2}} - \hat{f}_{i-\frac{1}{2}}) + \nu(u'_{i+\frac{1}{2}} - u'_{i-\frac{1}{2}}), \tag{5.3}$$

where $\bar{u}_i(t)$ is the numerical approximation to the cell average $\bar{u}(x_i, t)$ and the numerical flux $\hat{f}_{x_{i+1/2}}$ is defined by

$$\hat{f}_{i+\frac{1}{2}} = h(u_{i+\frac{1}{2}}^L, u_{i+\frac{1}{2}}^R). \tag{5.4}$$

The values of $u_{i+1/2}^{L,R}$ are reconstructed by using the HPUS scheme. The second-order Roe flux [43] is adopted for the present computation

$$\hat{f}_{i+\frac{1}{2}}^{Roe} = \frac{1}{2} \left[f(u_{i+\frac{1}{2}}^L) + f(u_{i+\frac{1}{2}}^R) - |a_{i+\frac{1}{2}}| (u_{i+\frac{1}{2}}^R - u_{i+\frac{1}{2}}^L) \right], \tag{5.5}$$

where

$$a_{i+\frac{1}{2}} = \begin{cases} \frac{f(u_{i+\frac{1}{2}}^R) - f(u_{i+\frac{1}{2}}^L)}{u_{i+\frac{1}{2}}^R - u_{i+\frac{1}{2}}^L}, & (u^R \neq u^L), \\ f'(u_{i+\frac{1}{2}}^L), & (u^R = u^L). \end{cases}$$

Algorithm 5.1 is presented below for the computational procedure of the scalar equation.

For the discretization of the diffusion term $u'_{i+1/2}$ with 3rd-order accuracy in the finite volume formulation, a polynomial of degree 3, $p(x)$, is to be reconstructed by using the four cell-average values $\bar{u}_{i-1}, \bar{u}_i, \bar{u}_{i+1}, \bar{u}_{i+2}$. When the polynomial reconstruction is considered, $p(x)$ should conform with the following relationship:

$$\frac{1}{\Delta x} \int_{j-\frac{1}{2}}^{j+\frac{1}{2}} p(x) dx = \bar{u}_j, \quad j = i - 1, i, i + 1, i + 2. \tag{5.6}$$

Algorithm 5.1 HPUS scheme for the scalar equation (5.1)

while ($0 < time < T$) **do**
 for $i = 1$ to N **do**
 if the reconstruction of $u_{i+1/2}^L$ **then**
 $u_U \leftarrow \bar{u}_{i-1}$
 $u_C \leftarrow \bar{u}_i$
 $u_D \leftarrow \bar{u}_{i+1}$
 Calculating the normalized value at the cell center $\hat{u}_C = \frac{u_C - u_U}{u_D - u_U}$
 The value of $u_{i+1/2}^L$ can be reconstructed by using the non-normalized HPUS scheme
 $u_{i+\frac{1}{2}}^L = u_U + (u_C - u_U)[-4(\frac{u_C - u_U}{u_D - u_U})^4 + 10(\frac{u_C - u_U}{u_D - u_U})^3 - 8(\frac{u_C - u_U}{u_D - u_U})^2 + (\frac{u_C - u_U}{u_D - u_U}) + 2], 0 < \hat{u}_C < 1$
 $u_{i+\frac{1}{2}}^L = u_C$, elsewhere
 end if
 if the reconstruction of $u_{i+1/2}^R$ **then**
 $u_U \leftarrow \bar{u}_i$
 $u_C \leftarrow \bar{u}_{i+1}$
 $u_D \leftarrow \bar{u}_{i+2}$
 Calculating the normalized value at the cell center $\hat{u}_C = \frac{u_C - u_U}{u_D - u_U}$
 The value of $u_{i+1/2}^R$ can be reconstructed by using the non-normalized HPUS scheme
 $u_{i+\frac{1}{2}}^R = u_U + (u_C - u_U)[-4(\frac{u_C - u_U}{u_D - u_U})^4 + 10(\frac{u_C - u_U}{u_D - u_U})^3 - 8(\frac{u_C - u_U}{u_D - u_U})^2 + (\frac{u_C - u_U}{u_D - u_U}) + 2], 0 < \hat{u}_C < 1$
 $u_{i+\frac{1}{2}}^R = u_C$, elsewhere
 end if
 Using the Roe flux (5.5) for the computation of the numerical fluxes $\hat{f}_{i+1/2}$ and $\hat{f}_{i-1/2}$
 end for
 Using the third-order TVD Runge-Kutta method for the time marching
 $time = time + \Delta t$
end while

These relationships can uniquely lead to a polynomial of degree 3

$$\begin{aligned}
 p(x) = & \frac{1}{12}(3\bar{u}_{i-1} + 13\bar{u}_i - 5\bar{u}_{i+1} + \bar{u}_{i+2}) \\
 & \frac{1}{12\Delta x}(-11\bar{u}_{i-1} + 9\bar{u}_i + 3\bar{u}_{i+1} - \bar{u}_{i+2})(x - x_{i-\frac{1}{2}}) \\
 & \frac{1}{4(\Delta x)^2}(3\bar{u}_{i-1} - 7\bar{u}_i + 5\bar{u}_{i+1} - \bar{u}_{i+2})(x - x_{i-\frac{1}{2}})^2 \\
 & \frac{1}{6(\Delta x)^3}(-\bar{u}_{i-1} + 3\bar{u}_i - 3\bar{u}_{i+1} + \bar{u}_{i+2})(x - x_{i-\frac{1}{2}})^3. \quad (5.7)
 \end{aligned}$$

The estimate of the cell-face slope $u'_{i+1/2}$ is give by

$$u'_{i+\frac{1}{2}} = p'(x_{i+\frac{1}{2}}) = \frac{1}{\Delta x} \left(\frac{1}{12}\bar{u}_{i-1} - \frac{5}{4}\bar{u}_i + \frac{5}{4}\bar{u}_{i+1} - \frac{1}{12}\bar{u}_{i+2} \right). \quad (5.8)$$

Acknowledgments

This work is supported by the National Natural Science Foundation of China (Grant No. 11061021) and Key Project of Chinese Ministry of Education (12024), the Scientific Research Projection of Higher Schools of Inner Mongolia (NJ10016, NJ10006, NJZZ12011) and the National Natural Science Foundation of Inner Mongolia Province (2011BS0102).

References

- [1] S. E. HARRIS, *Sonic shocks governed by the modified Burgers' equation*, Eur. J. Appl. Math., 7 (2) (1996), pp. 201–222.
- [2] P. L. SACHDEV AND CH. SRINIVASA RAO, *N-wave solution of modified Burgers' equation*, Appl. Math. Lett., 13 (2000), pp. 1–6.
- [3] P. L. SACHDEV, CH. SRINIVASA RAO AND B.O. ENFLO, *Large-time asymptotics for periodic solutions of the modified Burgers' equation*, Stud. Appl. Math., 114 (2005), pp. 307–323.
- [4] I. INAN AND Y. UGURLU, *Exp-function method for the exact solutions of fifth order KdV equation and modified Burgers' equation*, Appl. Math. Comput., 217 (2009), pp. 1294–1299.
- [5] M. A. RAMADAN AND T.S. EL-DANAF, *Numerical treatment for the modified Burgers' equation*, Math. Comput. Simul., 70 (2005), pp. 90–98.
- [6] M. A. RAMADAN, T.S. EL-DANAF AND F. ALAAL, *A numerical solution of the Burgers' equation using septic B-splines*, Chaos Solitons Fractals, 26 (2005), pp. 795–804.
- [7] I. DAČ, D. IRK AND B. SAKA, *A numerical solution of the Burgers' equation using cubic B-splines*, Appl. Math. Comput., 163 (2005), pp. 199–211.
- [8] I. DAČ, B. SAKA AND A. BOZ, *B-spline Galerkin methods for numerical solutions of the Burgers' equation*, Appl. Math. Comput., 166 (2005), pp. 506–522.
- [9] B. SAKA AND I. DAČ, *Quartic B-spline collocation methods to the numerical solutions of the Burgers' equation*, Chaos Solitons Fractals, 32 (2007), pp. 1125–1137.
- [10] B. SAKA AND I. DAČ, *A numerical study of the Burgers' equation*, J. Franklin Inst., 345 (2008), pp. 328–348.
- [11] D. IRK, *Sextic B-spline collocation method for the modified Burgers' equation*, Kybernetes, 38(9) (2009), pp. 1599–1620.
- [12] R. S. TEMSAH, *Numerical solutions for convection-diffusion equation using El-Gendi method*, Commun. Nonlinear Sci. Numer. Simul., 14 (2009), pp. 760–769.
- [13] Y. DUAN, R. LIU AND Y. JIANG, *Lattice Boltzmann model for the modified Burgers' equation*, Appl. Math. Comput., 202 (2008), pp. 489–497.
- [14] A. G. BRATSOS, *A fourth-order numerical scheme for solving the modified Burgers' equation*, Appl. Math. Comput., 60 (2010), pp. 1393–1400.
- [15] W. SHYY, *A study of finite difference approximations to steady-state, a convection-dominated flow problem*, J. Comp. Phys., 57 (1985), pp. 415–438.
- [16] B. P. LEONARD, *A stable and accurate modelling procedure based on quadratic interpolation*, Comput. Meth. Appl. Mech. Engng., 19 (1979), pp. 59–98.
- [17] R. K. AGARWAL, *A third-order-accurate upwind scheme for Navier-Stokes solutions at high Reynolds numbers*, AIAA paper 1981-112 in 19th AIAA Aerospace Sciences Meeting, St. Louis, MO, USA, (1981).

- [18] ABDULLAH SHAH, HONG GUO AND LI YUAN, *A third-order upwind compact scheme on curvilinear meshes for the incompressible Navier-Stokes equations*, Commun. Comput. Phys., 5 (2009), pp. 712–729.
- [19] P. D. LAX AND B. WENDROFF, *Systems of conservation laws*, Commun. Pur. Appl. Math., 13 (1960), pp. 217–237.
- [20] P. L. ROE, *Characteristic-based schemes for the Euler equations*, Ann. Rev. Fluid Mech., 18 (1986), pp. 337–365.
- [21] A. HARTEN, *High resolution schemes for hyperbolic conservation law*, J. Comp. Phys., 49 (1983), pp. 357–4393.
- [22] P. K. SWEBY, *High resolution schemes using flux limiters for hyperbolic conservation laws*, SIAM J. Numer. Anal., 21 (1984), pp. 995–1011.
- [23] B. VAN LEER, *Towards the ultimate conservative difference scheme monotonicity and conservation combined in a second-order scheme*, J. Comp. Phys., 14 (1974), pp. 361–370.
- [24] B. VAN LEER, *Upwind and high-resolution methods for compressible flow: From donor cell to residual-distribution schemes*, Commun. Comput. Phys., 1 (2006), pp. 192–206.
- [25] P. H. GASKELL AND A. K. C. LAU, *Curvature-compensated convective transport: SMART, a new boundedness-perserving transport algorithm*, Int. J. Numer. Meth. Fl., 8 (1988), pp. 617–641.
- [26] B. P. LEONARD, *Simple high-accuracy resolution program for convective modeling of discontinuities*, Int. J. Numer. Meth. Fl., 8 (1988), pp. 1291–1318.
- [27] J. ZHU, *A low-diffusive and oscillation-free convective scheme*, Comm. Appl. Mech. Eng., 7 (1991), pp. 225–232.
- [28] M. S. DARWISH *A new high-resolution scheme based on the normalized variable formulation*, Numer. Heat Trans. B, 24 (1993), pp. 353–337.
- [29] J. J. WEI, B. YU AND W. Q. TAO, *A new High-order-accurate and bounded scheme for incompressible flow*, Numer. Heat Trans. B, 43 (2003), pp. 19–41.
- [30] B. SONG , G. R. LIU , K.Y. LAM AND R.S. AMANO, *On a higher-order discretization scheme*, Int. J. Numer. Meth. Fl., 32 (2000), pp. 881–897.
- [31] M. A. ALVES , P. J. OLIVEIRA AND F. T. PINHO, *A convergent and universally bounded interpolation scheme for the treatment of advection*, Int. J. Numer. Meth. Fl., 41 (2003), pp. 47–75.
- [32] B. YU , W. Q. TAO, D. S. ZHANG AND Q. W. WANG, *Discussion on numerical stability and boundedness of convective discretized scheme*, Numer. Heat Trans. B, 40 (2001), pp. 343–365.
- [33] P. L. HOU , W. Q. TAO AND M. Z. YU, *Refinement of the convective boundedness criterion of Gaskell and Lau*, Eng. Comput., 20 (2003), pp. 1023–1043.
- [34] C-H. LIN AND C. A. LIN, *Simple high-order bounded convection scheme to model discontinuities*, AIAA J., 35 (1997), pp. 563–565.
- [35] H. LIN AND C. C. CHIENG, *A characteristic-based flux limiter of an essentially 3rd-order flux-splitting method for hyperbolic conservation laws*, Int. J. Numer. Meth. Fl., 13 (1991), pp. 287–301.
- [36] S. K. GODUNOV, *Finite difference method for numerical computation of discontinuous solutions of the equations of the fluid dynamics*, (in Russian), Mat. Sbornik, 47 (1959), pp. 271–306.
- [37] C. HIRSCH, *Numerical Computation of Internal and External Flows*, Wiley, New York (1990).
- [38] M. ZIJLEMA AND P. WESSELING, *Higher order flux-limiting methods for steady-state, multi-dimensional, convection-dominated flow*, Report 1995-131, Delft University of Technology.
- [39] I. A. HASSANIEN, A. A. SALAMA AND H. A. HOSHAM, *Fourth-order finite difference method for solving Burgers' equation*, Appl. Math. Comput., 170 (2005), pp. 781–800.

- [40] S. KUTLUAY, A. R. BAHADIR AND A. ÖZDES, *Numerical solution of one-dimensional Burgers' equation: explicit and exact-explicit finite difference method*, J. Comp. Appl. Math., 103 (1999), pp. 251–261.
- [41] M. XU, R. WANG, J. ZHANG AND Q. FANG, *A novel numerical scheme for solving Burgers' equation*, Appl. Math. Comput. (2010), (accepted).
- [42] V. G. FERREIRA, F. A. KUROKAWA AND R. A. B. QUEIROZ, *Assessment of a high-order finite difference upwind scheme for the simulation of convection-diffusion problems*, Int. J. Numer. Meth. Fl., 60 (2009), pp. 1–26.
- [43] P. L. ROE, *Approximate Riemann solvers, parameter vectors and difference schemes*, J. Comput. Phys., 43 (1980), pp. 357–372.
- [44] M. YANG, Z. J. WANG, *A parameter-free generalized moment limiter for high-order methods on unstructured grids*, Adv. Appl. Math. Mech., 4 (2009), pp. 451–480.
- [45] M. A. ALVES, P. J. OLIVEIRA, F. T. PINHO, *A convergent and universally bounded interpolation scheme for the treatment of advection*, Int. J. Numer. Meth. Fl., 41 (2003), pp. 47–75.
- [46] K. C. NG, M. Z. YUSOFF AND K. NG, *Higher-order bounded differencing schemes for compressible and incompressible flows*, Int. J. Numer. Meth. Fl., 53 (2007), pp. 57–80.